AIP | Journal of Applied Physics

Anomalous wear-out phenomena of europium-implanted light emitters based on a metal-oxide-semiconductor structure

L. Rebohle, J. Lehmann, S. Prucnal, A. Nazarov, I. Tyagulskii, S. Tyagulskii, A. Kanjilal, M. Voelskow, D. Grambole, W. Skorupa, and M. Helm

Citation: Journal of Applied Physics **106**, 123103 (2009); doi: 10.1063/1.3272781
View online: http://dx.doi.org/10.1063/1.3272781
View Table of Contents: http://scitation.aip.org/content/aip/journal/jap/106/12?ver=pdfcov
Published by the AIP Publishing

Articles you may be interested in

Comparison of electrical and electro-optical characteristics of light-emitting capacitors based on silicon-rich Si-oxide fabricated by plasma-enhanced chemical vapor deposition and ion implantation
J. Appl. Phys. **111**, 053109 (2012); 10.1063/1.3692082

The effect of rare-earth clustering on charge trapping and electroluminescence in rare-earth implanted metal-oxide-semiconductor light-emitting devices
J. Appl. Phys. **107**, 123112 (2010); 10.1063/1.3436591

Blue and red electroluminescence of Europium-implanted metal-oxide-semiconductor structures as a probe for the dynamics of microstructure
Appl. Phys. Lett. **93**, 071908 (2008); 10.1063/1.2964176

Switchable two-color electroluminescence based on a Si metal-oxide-semiconductor structure doped with Eu
Appl. Phys. Lett. **90**, 181121 (2007); 10.1063/1.2735285

Bright green electroluminescence from Tb 3 + in silicon metal-oxide-semiconductor devices
J. Appl. Phys. **97**, 123513 (2005); 10.1063/1.1935766

[This article is copyrighted as indicated in the article. Reuse of AIP content is subject to the terms at: http://scitation.aip.org/termsconditions. Downloaded to] IP: 129.21.35.191 On: Sat, 20 Dec 2014 17:09:12

Anomalous wear-out phenomena of europium-implanted light emitters based on a metal-oxide-semiconductor structure

L. Rebohle,[a)] J. Lehmann, S. Prucnal, A. Nazarov,[b)] I. Tyagulskii,[b)] S. Tyagulskii,[b)]
A. Kanjilal, M. Voelskow, D. Grambole, W. Skorupa, and M. Helm
Institute of Ion Beam Physics and Materials Research, Forschungszentrum Dresden Rossendorf e.V., P.O. Box 510119, 01314 Dresden, Germany

(Received 18 August 2009; accepted 11 November 2009; published online 23 December 2009)

The anomalous wear-out phenomena of Eu-implanted metal-oxide-semiconductor devices were investigated. It will be shown that in contrast to other rare earth elements the electroluminescence (EL) intensity of Eu-implanted SiO_2 layers can rise under constant current injection before the known EL quenching will start. Under certain circumstances, this rise may amount up to two orders of magnitude. The EL behavior will be correlated with the microstructural and electrical properties of the devices. Transmission electron microscopy and Rutherford backscattering spectroscopy were applied to trace the development of Eu/Eu oxide clusters and the diffusion of Eu to the interfaces of the gate oxide layer. The hydrogen profile within the SiO_2–SiON interface region was determined by nuclear reaction analysis. Current-voltage characteristics, EL decay times, and the progression of the voltage and the EL spectrum with increasing charge injection were measured to study charge and trapping phenomena in the oxide layer to reveal details of the EL excitation mechanism. A first qualitative model for the anomalous life time behavior is proposed. © *2009 American Institute of Physics*. [doi:10.1063/1.3272781]

I. INTRODUCTION

The motivation for Si-based photonics is clearly driven by the semiconductor and telecommunication industry which wants to overcome the limitations of a pure electronic data processing. The vision behind is the assembling of electrical and optical functions in one and the same chip. Whereas there are already satisfying solutions for a couple of integrated photonic devices such as detectors,[1] waveguides,[2] and modulators;[3,4] the most critical element is the electrically driven light emitter. Among the different approaches rare earth (RE) implanted metal-oxide-semiconductor (MOS) devices are of special interest as they combine the superior electric properties of the SiO_2–Si system with the excellent optical properties of RE elements. Electroluminescence (EL) from RE-implanted MOS structures was shown for a couple of RE elements.[5–12] In Ref. 9, we were able to demonstrate an external quantum efficiency of 16% for Tb-implanted MOS light emitting devices (MOSLEDs), whereas Gd implantation into SiO_2 results in an intense single and sharp UV line at 316 nm.[10] First investigations on Eu-implanted SiO_2 layers[11,12] revealed that the EL spectrum is very sensitive to the implantation, annealing, and electrical operation conditions with the latter case enabling the construction of a multicolor device in which the color depends on the injection current.

However, despite these respectable successes, none of these light emitters can compete at present with III-V light emitters or organic LEDs in terms of efficiency and lifetime. In order to improve the performance of RE-implanted MOSLEDs, a deeper insight about the ongoing processes in the active layer of the light emitter is indispensable, which especially applies for EL quenching and oxide degradation processes. Recently it was shown that the EL intensity of RE-implanted MOSLEDs under constant current injection shows a constant plateau phase followed by EL quenching,[13] which was explained by electron trapping caused by traps with a small capture cross section. In comparison to other RE elements, Eu exhibits a much stronger electron trapping which was correlated with an enhanced and accelerated Eu/Eu oxide cluster growth during annealing.[14]

In this paper, we will demonstrate another particular feature of Eu-implanted SiO_2 layers which exhibit a rise of the EL intensity under constant current injection—up to two orders of magnitude in the extreme case—before the known EL quenching will start. The EL data will be correlated with the electrical and microstructural properties of the devices, and based on these results a first qualitative model for the anomalous wear-out behavior of Eu-implanted SiO_2 layers is proposed. In the case of EL, we confine the discussion to the red EL around 618 nm which is very indicative for Eu^{3+} and therefore very suitable for the correlation with other properties. Moreover, the usual operation conditions for optical and electrical investigations, namely, low and medium injection currents,[11] favor the red EL. Beside the strong scientific interest, the EL rise phenomenon has the potential for significant improvements of the device performance. If the process is sufficiently understood and can be somehow controlled, it can be used to compensate the normal EL quenching process resulting in an adequate increase of the device lifetime.

[a)]Author to whom correspondence should be addressed. Electronic mail: l.rebohle@fzd.de.
[b)]Also at Lashkaryov Institute of Semiconductor Physics, National Academy of Sciences of Ukraine, Prospect Nauky 45, 03028 Kiev, Ukraine.

 © 2009 American Institute of Physics

[This article is copyrighted as indicated in the article. Reuse of AIP content is subject to the terms at: http://scitation.aip.org/termsconditions. Downloaded to] IP: 129.21.35.191 On: Sat, 20 Dec 2014 17:09:12

II. EXPERIMENTAL

The Eu-implanted MOS structures were fabricated by local oxidation of silicon (LOCOS) with 100 nm thick thermally grown SiO_2 layer on {100} oriented n-type silicon wafers. This layer was implanted with 100 keV Eu ions to doses of 2×10^{14}, 1×10^{15}, and 3×10^{15} cm^{-2}, which should result according to SRIM calculations[15] in a Gaussian-like implantation profile in the middle of the oxide layer with Eu peak concentrations of about 0.1, 0.5, and 1.5 at. %, respectively. Please note that already the as-implanted Eu profile as calculated from the Rutherford-backscattering (RBS) random spectrum shows a lower total Eu concentration in the order of 80%–90% of the nominal dose and a slight broadening of the profile in comparison to the SRIM calculations which is accompanied by an adequate reduction in the peak concentration down to 60% of the nominal value in the extreme case. This is most probable due to implantation-induced diffusion processes which may occur under high implantation currents. Nevertheless, the value of the nominal peak concentration is used in the following to avoid confusion. The implantation is followed by flash lamp annealing (FLA) for 20 ms, rapid thermal annealing (RTA) for either 6 or 60 s, and furnace annealing (FA) for 30 min in a nitrogen ambient at temperatures between 800 and 1000 °C. The device structures are finally supplied with a 100 or 200 nm thick SiON protection layer fabricated by plasma enhanced chemical vapor deposition (PECVD) at 300 °C, a transparent front contact made of indium-tin oxide and a rear contact made of aluminum. For microstructural investigations, flat structures without LOCOS and without an upper electrode were fabricated.

The microstructure was investigated by transmission electron microscopy (TEM) under cross sectional geometry with a FEI-Titan 80-300 S/TEM operating at 300 kV, by RBS using 1.7 MeV He ions and by nuclear reaction analysis (NRA) exploiting the resonant reaction ^{15}N (6.385 MeV) $+{}^{1}H\rightarrow{}^{12}C+{}^{4}He+\gamma$-rays (4.43 MeV). The hydrogen depth profile is determined by gradually increasing the incident energy of ^{15}N ions and thus moving the resonance at 6.385 MeV progressively to greater depths. Current-voltage (IV) characteristics were recorded by using a Keithley 2410 source measurement unit which served as a current source for the other electric measurements as well. For ΔV_{CC} measurements, a constant current is injected into the devices, while the change in the applied voltage is monitored as a function of time. The EL was obtained by applying a constant current of 5 μA to circular dots with a diameter of 300 μm and a Shamrock monochromator in combination with a spectroscopic charge coupled device camera which allowed the continuous recording of EL spectra with time. The EL spectra were corrected for the device function of the detection system. Finally, the EL decay time was measured by a multichannel scalar (Stanford Research System SR430) under constant voltage pulses.

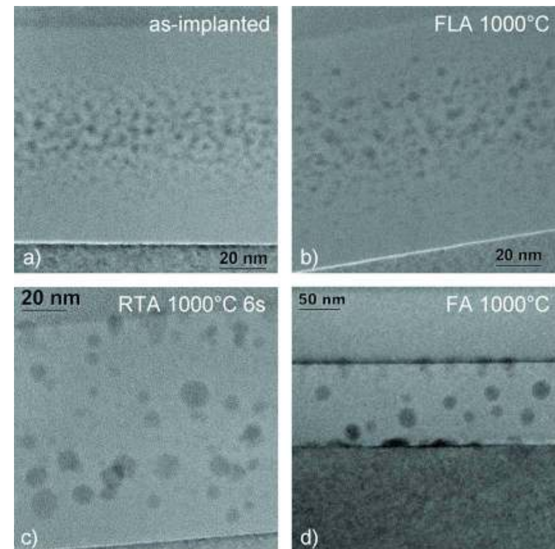

FIG. 1. (Color online) Bright field XTEM images showing the gate oxide layer of Eu-implanted MOSLEDs together with its interfaces to Si (bottom) and SiON (up). Please note the different magnification for FA 1000 °C.

III. RESULTS AND DISCUSSION

A. Microstructure

The development of the microstructure strongly depends on the thermal budget applied to the structure during annealing. Figure 1 traces this development by showing a sequence of TEM images of Eu-implanted MOSLEDs in the as-implanted stage and annealed at 1000 °C with increasing annealing time. The images exhibit the Eu-implanted SiO_2 layer with the adjacent Si substrate and the SiON layer at the bottom and the upper part of the images, respectively. In the as-implanted stage [Fig. 1(a)], small amorphous clusters with a size around 3–4 nm can already be found in the middle of the SiO_2 layer. As briefly discussed in Sec. II, this cluster formation is also assumed to be caused by implantation-induced diffusion processes. At present it is not yet clear if the clusters are composed of Eu, EuO, Eu_2O_3, or a mixture of them. However, based on the thermodynamic properties of Eu, namely, the formation enthalpy of the Eu oxides, we assume that Eu tends to cluster in an oxidized form.[12] Moreover, in the rare case where crystalline clusters are observed (RTA 1000 °C 6 s) using high-resolution TEM, the interplanar spacing obtained by Fourier transformation of the atomic planes of such crystallites confirms the formation of the Eu_2O_3 phase.

Whereas FLA 1000 °C [Fig. 1(b)] does not change the picture very much, at RTA 1000 °C 6 s [Fig. 1(c)], the formation of larger clusters at the expense of smaller ones caused by Ostwald ripening can be observed. In addition, there is also a significant diffusion of Eu to the interfaces of the SiO_2 layer which becomes evident by the first Eu segregations at the interfaces and by the broadened cluster band now extending across the whole oxide layer. In case of FA 1000 °C [Fig. 1(d)], the TEM images show large amorphous clusters up to 20 nm in size and SiO_2 interfaces which are heavily decorated with Eu. At the $Si-SiO_2$ interface even the dissolution of large clusters can be observed which may oc-

[This article is copyrighted as indicated in the article. Reuse of AIP content is subject to the terms at: http://scitation.aip.org/termsconditions. Downloaded to] IP: 129.21.35.191 On: Sat, 20 Dec 2014 17:09:12

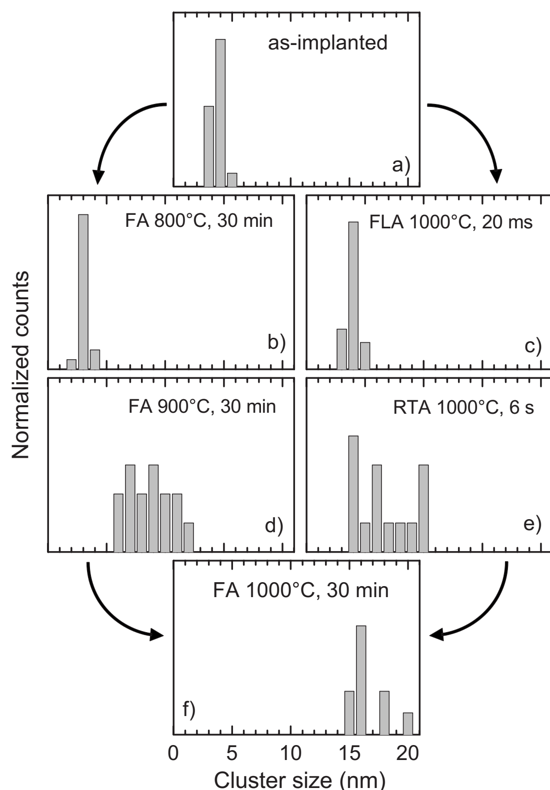

FIG. 2. Cluster size distribution of Eu/Eu oxide clusters as a function of the annealing temperature (left column) and the annealing time (right column). The cluster sizes were determined manually from the XTEM images shown in Fig. 1.

cur in the framework of Ostwald ripening with the Si–SiO_2 interface representing the surface of an "infinite" large cluster. Eu/Eu oxide clusters may grow up in the vicinity of this interface, but if they are large enough Eu diffusion from these clusters to the nearby interface becomes dominant resulting in the dome-shaped structures seen in Fig. 1(d).

A similar development is also found for increasing annealing temperatures. In Fig. 2 the development of the size distribution of the clusters with increasing annealing time at 1000 °C is compared with the cluster development with increasing annealing temperature. Although the cluster sizes were determined manually from the TEM images resulting in an uncertainty of 1–2 nm, the general tendency is obvious. If the thermal budget exceeds a certain limit either by high temperature or long annealing times, a strong Eu diffusion starts which finally ends up with the structure known for FA 1000 °C with large Eu clusters and strong Eu segregations at the interfaces. The transition points, namely, FA 900 °C and RTA 1000 °C 6 s, appear to be equivalent.

The redistribution of the implanted Eu can be quantified by RBS measurements, as shown in Fig. 3. Whereas the implanted Eu profiles after FA 800 °C and FLA 1000 °C look very similar to the as-implanted profile, at FA 900 °C or RTA 1000 °C 6 s first agglomerations of Eu are visible at the SiO_2–SiON interface. Eu segregations at the Si–SiO_2 interface are not yet visible, but with increasing annealing temperature and/or annealing time the Eu diffusion becomes more intense, and at FA 1000 °C the amount of Eu at both interfaces is higher than in the middle of the oxide layer. If

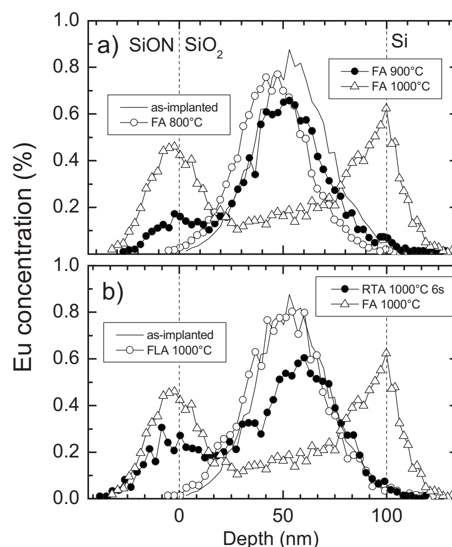

FIG. 3. Elemental depth profiles calculated from RBS spectra for Eu in SiO_2 layers implanted with a nominal dose of 3×10^{15} cm^{-2} and annealed with different annealing temperatures (a) and different annealing times (b). An atomic density of 6.6×10^{22} cm^{-3} has been assumed for the SiO_2 layer in order to calculate the depth scale.

the middle of the oxide layer is defined as the region between 20 and 80 nm of the depth scale in Fig. 3, only 34% of the implanted Eu can be found within this region.

There is another important change in the microstructure which is not visible in TEM or RBS but is of special interest for the later discussion of charge trapping in MOSLED structures. This is the amount of hydrogen which is introduced into the system during the SiON layer deposition and which can be measured by NRA. Figure 4 shows the concentration of hydrogen measured in this way as a function of depth around the SiO_2–SiON interface. In all cases the hydrogen profiles are characterized by a nearly constant concentration in the SiON layer, which drops down at the SiO_2–SiON interface by a factor of 3–10 depending on the type of annealing. Whereas in the as-implanted stage a hydrogen concentration of about 18% is measured in the SiON layer, this value decreases to 3% and 0.2% in the cases of FLA 1000 °C and FA 1000 °C, respectively. The comparison be-

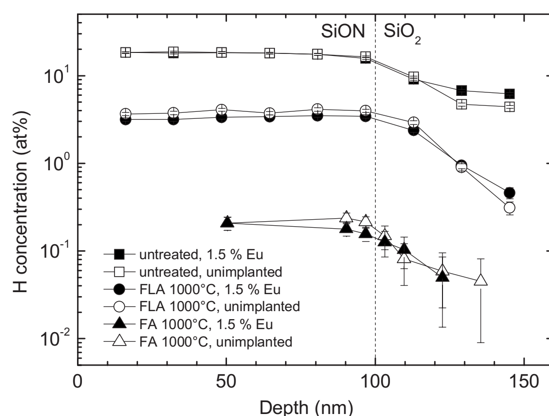

FIG. 4. Elemental depth profiles of hydrogen in unimplanted and Eu-implanted MOSLEDs as derived from NRA. A SiO_2 density of 2.2 g cm^{-3} and an average energy loss of 1.55 keV/nm have been assumed in order to calculate the depth scale.

[This article is copyrighted as indicated in the article. Reuse of AIP content is subject to the terms at: http://scitation.aip.org/termsconditions. Downloaded to] IP: 129.21.35.191 On: Sat, 20 Dec 2014 17:09:12

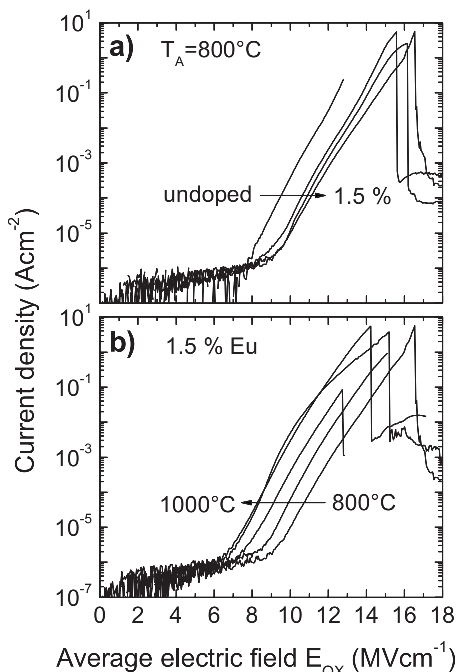

FIG. 5. IV characteristics of Eu-implanted SiO_2 layers with 0.1%, 0.5%, and 1.5% of Eu in comparison with the unimplanted SiO_2 (a). All devices were annealed with FA 800 °C. In the lower diagram, the shift of the IV characteristics from devices containing 1.5% Eu with increasing annealing temperature is shown (b).

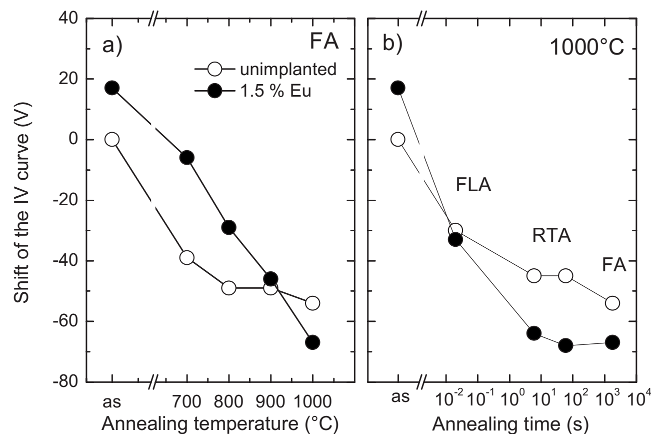

FIG. 6. Shift of the IV characteristics of unimplanted (open circles) and Eu-implanted MOSLEDs with 1.5% Eu (closed circles) relative to the unimplanted, untreated device as a function of annealing temperature (a) and annealing time (b). Untreated MOSLEDs—independent whether they are implanted or not—are labeled with "as."

tween Eu-implanted MOSLEDs (closed symbols) and unimplanted MOSLEDs (open symbols) reveals that (i) the hydrogen content strongly decreases with an increasing thermal budget and (ii) that this process is entirely independent of whether the MOSLED was implanted or not. The first item is well known from literature; e.g., in investigations comparing the properties of silicon nitride layers deposited by PECVD and low pressure chemical vapor deposition (LPCVD), it was found that the hydrogen content drops below 3% if the deposition temperature exceeds 700 °C.[16] The second behavior implies that the charge trapping of the MOSLEDs is composed of two parts: charge trapping, which is mainly due to hydrogen and thus depends only on the annealing conditions, and charge trapping, which is an effect of the Eu implantation.

B. Current-voltage characteristics

The IV characteristics of MOSLEDs, as shown in Fig. 5, follow the well-known pattern of Fowler–Nordheim (FN) tunneling (e.g., in Ref. 17) with very low injection currents at low electric fields, a roughly exponential growth of the injection current in the midfield region and a final breakdown at high electric fields. As the breakdown is a statistical event, the specific electric field initiating the breakdown may fluctuate. MOSLEDs are not ideal MOS devices, and consequently the FN curve is distorted by at least two processes. First of all, if there is a sufficient high number of traps in the $Si-SiO_2$ interface region, they can assist the FN tunneling by trap assisted tunneling. This might be especially the case for FA 1000 °C where extensive Eu segregations are found at the $Si-SiO_2$ interface. The second process is charging which deforms the SiO_2 conduction band and thus influences the local electric field at the injecting interface. Both processes cause a shift of the IV curve to lower or higher voltages depending on the type of the trapped charge carriers which appears as a lowering or an enhancement of the effective injection barrier. A third process—which is not further discussed in this article—is the possibility of charging *during* the IV measurement which can lead to deformations of the IV curve at very high injection currents.

Figure 5 displays the IV characteristics of the MOSLEDs for different Eu concentrations (a) and annealing temperatures (b) in a generalized form where the injection current density is plotted versus the average electric field in the oxide layer. Note that this average field was derived by splitting the applied voltage between the SiON and the SiO_2 layer considering relative dielectric constants of 7.2 and 3.9, respectively.[18] The given electric field is also the average over local electric fields which may vary due to charging effects in the oxide layer, especially at high injection currents. In Fig. 5(a), a shift of the IV curves to higher electric fields with increasing Eu concentration is observed for FA 800 °C. However, for a fixed Eu concentration, the IV curves shift to lower electric fields with increasing annealing temperature [Fig. 5(b)].

A tendency similar to the annealing temperature dependence can be observed for the annealing time dependence. In Fig. 6, these dependencies are compared with each other and with the unimplanted case by showing the shift of the IV characteristics in relation to an unimplanted, untreated (not annealed) MOSLED structure. Untreated MOSLEDs—independent whether they are implanted or not—are labeled with "as" in Fig. 6. For a better comparability with the following section, the shifts are expressed now as a voltage shift. Starting the discussion with the unimplanted case, it can be clearly seen that the IV characteristics shift to lower voltages (and thus lower electric fields) with increasing thermal budgets and reach a saturation value for either FA 800 °C or RTA 1000 °C 6 s. The FN fit of the IV characteristic for the unimplanted device annealed with FA 1000 °C

[This article is copyrighted as indicated in the article. Reuse of AIP content is subject to the terms at: http://scitation.aip.org/termsconditions. Downloaded to] IP: 129.21.35.191 On: Sat, 20 Dec 2014 17:09:12

gives reasonable values for the injection barrier around 3 eV without assuming additional charges, for which reason this device is regarded as being quite close to an ideal MOS structure. The shift of the IV characteristics can be correlated with the hydrogen content which is high for the untreated MOSLED and very low for FA 1000 °C (Fig. 4). It seems that hydrogen introduces negative charges which complicate the further injection of electrons. Please note that the shift of the IV characteristic itself depends on the product of charge and charge centroid, which is why no statement about the charge location can be made. For an analytical expression of these shifts, we refer to literature.[17]

In the case of Eu implantation, additional negative charges are introduced into SiO_2 causing an even larger shift of the IV curves to *higher* voltages in the as-implanted stage. With increasing thermal budget, the shift of the IV curves of Eu-implanted MOSLEDs is still larger than that of unimplanted MOSLEDs, but this trend is compensated at first and then turned into the opposite where the IV curves of Eu-implanted MOSLEDs show now a larger shift to *lower* voltages for high thermal budgets. As the additional negative charge in the as-implanted stage is directly connected with the Eu-implantation the charge centroid is assumed to be located around the projected range of the implanted element. With annealing three different processes will take place: (i) annealing of implantation-induced defects, (ii) cluster formation and growth, and (iii) Eu diffusion toward the interfaces. The development of the cluster size distribution in Fig. 2 reveals that there are no changes for low thermal budgets: FA 800 °C and FLA 1000 °C [Figs. 2(b) and 2(c)] do not differ significantly from the as-implanted stage [Fig. 2(a)]. However, in Fig. 6(a) the difference between Eu-implanted and unimplanted MOSLEDs is nearly the same for FA 800 °C and the as-implanted stage. In contrast to this, Eu-implanted and unimplanted MOSLEDs feature the same IV shift for FLA 1000 °C indicating that the additional negative charge introduced by Eu implantation has been disappeared [Fig. 6(b)]. Therefore, this initial negative charge is attributed to implantation-induced defects as the annealing of such defects often requires a local rearrangement of the electronic structure such as bond formation or relaxation. Such processes need a sufficiently high temperature for activation but take place on a much shorter time scale than diffusion. Applied to the present case, this implies that FA 800 °C is—regardless of the long annealing time—not sufficient to anneal out the majority of the implantation-induced defects, but FLA 1000 °C is.

For high thermal budgets, the shift of the IV characteristics to lower voltages is larger for Eu-implanted MOSLEDs than that for unimplanted MOSLEDs indicating that Eu leads now to additional positive charges in the dielectric layers. Close inspection of Fig. 6 reveals that this is the case for RTA and FA 1000 °C, which are both characterized by medium-sized or large clusters [Figs. 2(e) and 2(f)]. Another correlation is the diffusion of Eu toward the interfaces. However, the comparison of Figs. 3(b) and 6(b) reveals that RTA 1000 °C 6 s and FA 1000 °C induce nearly the same shift of the IV curve but differ strongly regarding the amount of Eu at the $Si-SiO_2$ interface. Therefore, it seems to be feasible

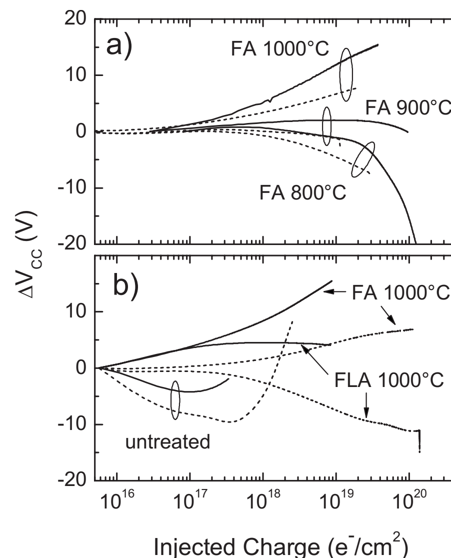

FIG. 7. Change of the applied voltage (ΔV_{CC}) under constant current injection for unimplanted (dashed line) and Eu-implanted MOSLEDs with 1.5% Eu (solid line) as a function of the annealing temperature (a) and the annealing time (b).

that the additional shift of the IV curve to lower voltages in the case of Eu is not caused by a lowering of the injection barrier due to Eu segregations, but originate from additional positive charges which are connected with larger clusters. However, as the behavior of FN tunneling and trap assisted tunneling is similar, it cannot be excluded that trap assisted tunneling gives a contribution to the IV shift in the case of FA 1000 °C. The reason why FA 900 °C having medium-sized clusters according to Fig. 2 does not show the same additional IV shift to lower voltages as RTA 1000 °C is not really known, but a speculative idea could be that, in fact, the positive charges are already present but compensated by the negative charge of implantation-induced defects which are not yet annealed out completely.

C. Charge trapping under constant current injection

Figure 7 displays the change of the applied voltage (ΔV_{CC}) under constant current injection for Eu-implanted (solid lines) and unimplanted MOSLEDs (dashed lines) for various annealing conditions. Similar to the IV measurements, the ΔV_{CC} characteristics can give certain information on the trapped charge and how it changes with time. The unimplanted untreated MOSLED exhibits a decrease in ΔV_{CC} up to a charge of $\sim 5 \times 10^{17}$ e^-/cm^2 which is usually interpreted as the buildup of a positive charge or as the reduction in a trapped negative charge. For higher charges a strong electron trapping is observed followed by an early breakdown. The situation changes already by applying a low thermal budget (FLA 1000 °C or FA 800 °C). In both cases ΔV_{CC} remains constant up to $\sim 5 \times 10^{17}$ e^-/cm^2 followed by a more moderate decrease in ΔV_{CC}. At high thermal budgets (FA 1000 °C), only a slight but constant increase in ΔV_{CC} indicating a moderate electron trapping is observed.

The behavior of the unimplanted MOSLEDs can be clearly correlated with the hydrogen content and the IV data. The shift of the IV curve to higher voltages [Fig. 6(b)] is the

[This article is copyrighted as indicated in the article. Reuse of AIP content is subject to the terms at: http://scitation.aip.org/termsconditions. Downloaded to] IP: 129.21.35.191 On: Sat, 20 Dec 2014 17:09:12

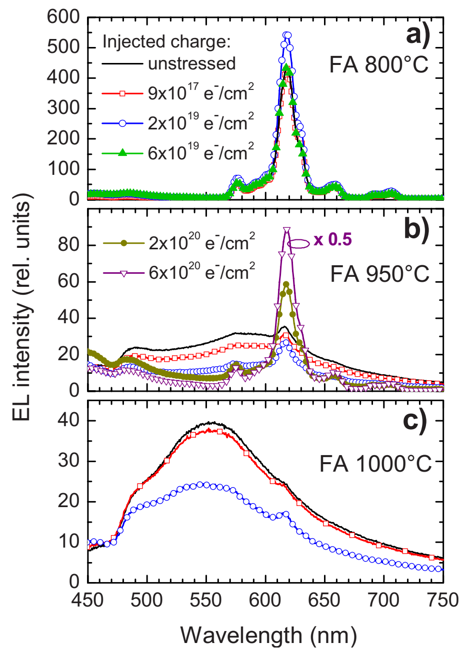

FIG. 8. (Color online) EL spectrum of MOSLEDs containing 1.5% Eu and annealed with FA at 800 °C (a), 950 °C (b), and 1000 °C (c) for various levels of charge injection. The EL spectra were taken during charge injection under a constant current density of 7 mA/cm^2.

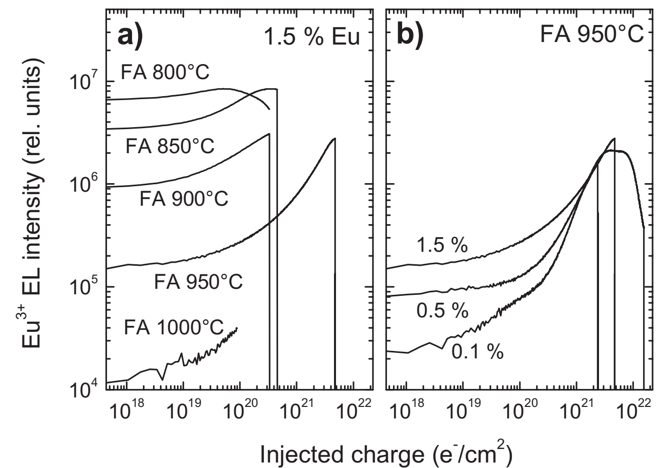

FIG. 9. Integrated Eu^{3+} EL intensity as a function of the injected charge for MOSLEDs implanted with 1.5% Eu and annealed at different temperatures (a) and for MOSLEDs annealed with FA 950 °C having different Eu concentrations (b).

larger the higher the amount of hydrogen found in the MOSLED (Fig. 4). According to Ref. 19, this behavior can be explained by the following oxide degradation mechanism. Under high electric fields, electrons moving in the conduction band of SiO_2 will be accelerated resulting in an equilibrium distribution of the kinetic energy of these electrons with average energies in the range 3–5 eV.[20] If these electrons approach the SiO_2–SiON interface, their kinetic energy is high enough to release hydrogen from interface trapping sites.[19] The released hydrogen can diffuse most probably in form of protons toward the Si–SiO_2 interface with either being trapped in the bulk building up a positive charge or being accumulated at the interface. However, as the charge centroid is not known the decrease in ΔV_{CC} can be the result of both a positive charge buildup and a reduction in the negative charge introduced originally by hydrogen.

The Eu implantation introduces additional electron traps leading to an additional buildup of negative charges and thus to an additional increase in ΔV_{CC} which is independent of the specific type of the applied annealing procedure. This implies also that the trapping properties of the Eu-related traps do not depend whether the Eu is present in the form of small clusters (as-implanted and low thermal budgets) or is accumulated in large clusters and at the interfaces (FA 1000 °C). Independent of the specific form, Eu is therefore associated with electron trapping during charge injection in the range of the observed injected charges. Please note that the ΔV_{CC} curves of MOSLEDs with other annealing conditions arrange according to the annealing temperature or time.

D. Evolution of the EL spectrum with time

Figure 8 traces the evolution of the EL spectrum of MOSLEDs containing 1.5% Eu with time under a constant current injection of 5 μA. First of all, the spectra of MOSLEDs annealed with FA 800 °C show the known signature of Eu^{3+} ions in the form of a main peak around 618 nm and satellites around 580, 660, and 700 nm which are due to 4f-intershell transitions from the $^5D_0$ level to some ^7F_J sublevels. For further spectroscopic details, we refer to the literature.[11,12,21]

In the case of FA 800 °C, the shape of the EL spectrum does not change very much with continuing charge injection. However, the intensity of the red EL caused by Eu^{3+} increases up to an injected charge of 2×10^{19} e^-/cm^2, followed by a smooth decrease for higher injected charges. In maximum, the gain of EL intensity compared to the initial value amounts to approximately 30%. Note that in Fig. 8(a) the curves for the virgin (unstressed) spectrum and those after charge injections of 9×10^{17} and 6×10^{19} e^-/cm^2 are superimposed. A similar behavior can be observed for FA 850 and 900 °C and for concentrations of 0.5% and 0.1% (not shown), but at 950 °C the figure will change. The unstressed spectrum shows a broad EL band of low intensity extending from the blue-green up to red with a small Eu^{3+} peak on top of it [Fig. 8(b), unstressed spectrum]. With continuing charge injection, the broad EL band gradually vanishes, and the red Eu^{3+} peak increases with time. In the case of FA 1000 °C [Fig. 8(c)], the red Eu^{3+} peak is hard to detect at the beginning but starts to rise with time, too. Unfortunately the stability was not high enough to observe a more spectacular outgrow of the red EL. It has to be noted that a similar but weaker behavior as in Fig. 8(b) can be observed already in the case of FA 900 °C, 0.1%. It is therefore assumed that the broad EL band is generally present at FA 900 °C, but with minor intensity and superimposed by the much stronger signal from Eu^{3+} in the cases of 0.5% and 1.5% Eu. It is well established in literature[22] that there is excess Si at the interface between thermally grown SiO_2 and Si_3N_4. This also accounts for the SiO_2–SiON interface and may contribute to the observed EL by oxygen deficiency centers which are known to show EL in the blue.[23]

Figure 9 shows the integral over the red Eu^{3+} peak at

[This article is copyrighted as indicated in the article. Reuse of AIP content is subject to the terms at: http://scitation.aip.org/termsconditions. Downloaded to] IP: 129.21.35.191 On: Sat, 20 Dec 2014 17:09:12

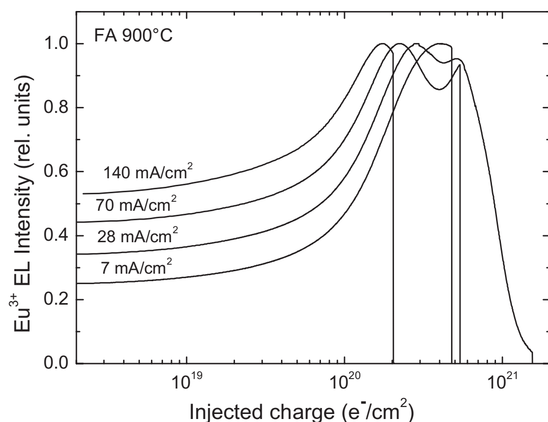

FIG. 10. Normalized, integrated Eu^{3+} EL intensity as a function of the injected charge for FA 900 °C and 0.1% Eu and its dependence on the injection current density.

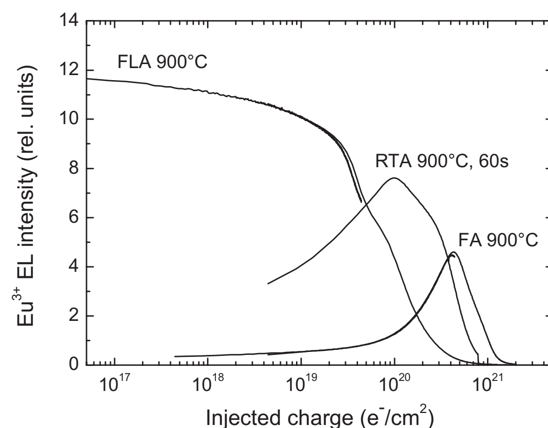

FIG. 11. Integrated Eu^{3+} EL intensity as a function of the injected charge for Eu-implanted MOSLEDs and different types of annealing. The injection current density is 7 mA/cm^2. Two characteristics are composed of two curves in order to cover a larger range of injected charges.

618 nm as a function of the injected charge for an injection current density of 7 mA/cm^2 (5 μA) and for Eu-implanted MOSLEDs with different annealing temperatures (a) and different Eu concentrations (b). The integral was corrected by background subtraction which is of special importance in the case of higher annealing temperatures. This type of representation with the intensity of the main emission line of a light emitter as a function of the injected charge will be denoted as a lifetime characteristic in the following. In general, the EL intensity of the red Eu^{3+} peak increases from an initial EL intensity value EL_0 with increasing injected charge, reaches a maximum at an injected charge Q_{inj}^{max}, and is finally quenched for very high injected charges. If the ratio between the maximum EL intensity achieved at Q_{inj}^{max} and EL_0 is denoted as θ the following tendencies can be observed: With increasing annealing temperature, EL_0 decreases strongly but is accompanied by a strong increase in θ which can reach a value of 100 in case of 0.1% Eu and FA 950 °C, as shown in Fig. 9(b). With increasing Eu concentration, EL_0 increases with an adequate decrease in θ. Whether there is a dependence of Q_{inj}^{max} on the Eu concentration is difficult to say as in many cases the MOSLEDs were not stable enough to show the whole range of the lifetime characteristic.

The next question is to which extent the lifetime characteristic of the Eu-implanted MOSLEDs depends on the injection current. Figure 10 displays the lifetime characteristics of a MOSLED with 0.1% Eu for different injection current densities and normalized with respect to the maximum EL intensity for better projection. First of all, the general shape of the lifetime characteristic is not changed very much, but there is a shift of Q_{inj}^{max} to smaller injected charges with increasing injection currents. However, this shift is quite small: the increase in the current density by a factor of 20 leads to a shift of Q_{inj}^{max} by a factor of something more than 2. Apparently, with increasing injection current an enhanced light emitting is observed, but the increase in EL_0 is accompanied by a decrease in θ.

Another interesting feature can be observed by comparing the lifetime characteristics of devices processed with different types of annealing, as shown in Fig. 11. For FLA 900 °C the curve starts with a high EL_0 value but decreases continuously with increasing injected charge. For RTA 900 °C, 60 s a maximum at $Q_{inj}^{max} \approx 10^{20}$ e$^-$/cm^2 can be observed which is shifted to larger injected charges for FA 900 °C. It seems that the anomalous behavior of the lifetime characteristic is closely linked with high thermal budgets, whereas low thermal budgets like FLA lead to the usual quenching behavior of RE-implanted MOSLEDs.

E. Qualitative model of the EL rise phenomenon

In Fig. 12, the lifetime characteristics of various RE-implanted MOSLEDs for constant current injection are shown. Except Eu the RE-implanted SiO_2 layers exhibit a smooth but continuous decrease in the EL intensity with increasing injected charge after an initial plateau phase of stable EL intensity. In former investigations, it was found that EL quenching is mainly attributed to electron trapping and the additional trap formation under constant current injection.[13] In contrast, the lifetime characteristic of the Eu-implanted MOSLEDs can be divided into two different phases: an initial *rise phase* and a subsequent *quenching phase*. Whereas the quenching phase is assumed to be caused by the same degradation processes as in the case of other RE-implanted MOSLEDs, the rise phase is surprising and

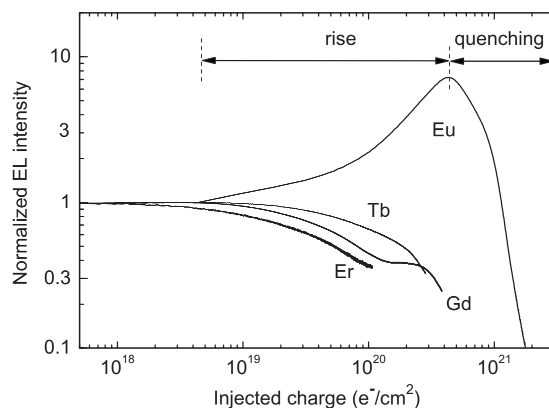

FIG. 12. Normalized EL intensity for RE-implanted MOSLEDs as a function of the injected charge.

[This article is copyrighted as indicated in the article. Reuse of AIP content is subject to the terms at: http://scitation.aip.org/termsconditions. Downloaded to] IP: 129.21.35.191 On: Sat, 20 Dec 2014 17:09:12

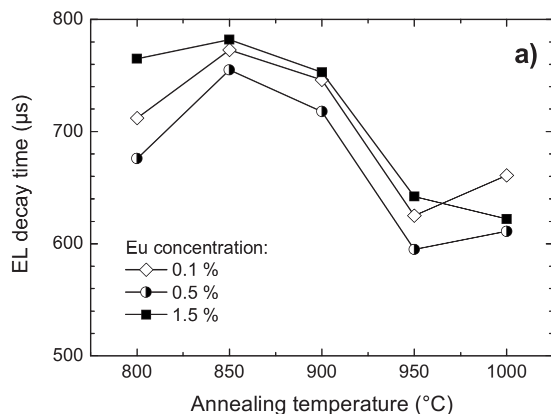

FIG. 13. EL decay times of Eu-implanted MOSLEDs as a function of Eu concentration and annealing temperature.

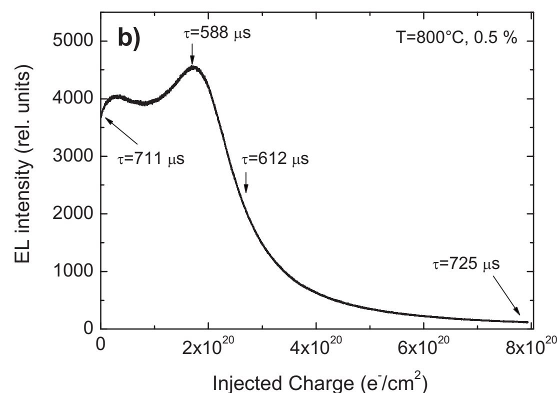

FIG. 14. EL intensity of a Eu-implanted MOSLED annealed by FA 800 °C and containing 0.5% Eu. After certain levels of charge injection, EL decay time measurements were performed whose decay times are assigned by arrows to the corresponding points of the EL intensity curve.

not known from other RE. Therefore, the following discussion will focus on this point.

If a rise of EL intensity with increasing injected charge is observed, the possible mechanism can be assigned in principle to one of the following categories:

(a) The number of Eu^{3+} ions is increasing during injection.
(b) A nonradiative decay path changes in intensity and decreases the degree of EL quenching during injection.
(c) The excitation of the Eu^{3+} ions becomes more efficient during injection.

Starting the discussion with category (a), it has to be stated first that all structural processes requiring high temperatures, namely, diffusion and cluster formation, are unlikely to occur with noteworthy intensity. It has to be assumed that the microstructure of the unstressed device in terms of Eu distribution, cluster size, and interface agglomerations remains unchanged during the whole period of charge injection. However, the number of Eu^{3+} ions may change due to recharging processes. Indeed, Eu can be present both in the divalent and trivalent ionic states, and depending on the Eu concentration and the annealing conditions a partially strong blue EL was found in Eu-implanted structures which was attributed to Eu^{2+} ions.[12] If this scenario would be of significance, Eu^{2+} ions have to transform into Eu^{3+} ions in order to cause the observed rise of the red EL intensity. There are two counterarguments. First, the unstressed structure in our case should exhibit a strong blue EL, especially in the case of FA 950 °C, which was not observed. Second, during the rise phase a concurrent increase in both the blue and red EL was observed for some MOSLEDs.

EL decay time measurements are the most suitable method to check if a change in the luminescence intensity is caused by the change of nonradiative decay paths [category (b)]. Figure 13 shows that the decay times of the unstressed devices exhibit a weak but significant dependence on the annealing temperature. In Fig. 14, the EL decay time values after certain levels of charge injection are given and correlated with the corresponding lifetime characteristic. If the EL is quenched by nonradiative decay paths, the corresponding decay time should decrease by the same factor as the EL intensity does. However, in our case decay times between 580 and 730 μs for the red $^5D_0$-$^7F_2$ line are measured, although the EL intensity drops down by a factor of nearly 40 if the injected charge increases from 2×10^{20} to 8×10^{20} e^-/cm^2. Moreover, close inspection of Fig. 14 reveals that the EL intensity increases up to an injected charge of 2×10^{20} e^-/cm^2, whereas the decay time shortens from 711 to 588 μs. We therefore conclude that nonradiative decay paths give only a minor contribution to the observed rise phase of the EL spectrum evolution.

The remaining potential mechanism [category (c)] for the EL rise phenomenon, namely, the increase in the Eu^{3+} excitation efficiency during the rise phase, should be now illuminated in detail. The present data are not sufficient to verify a definite mechanism, but based on the correlations between microstructure and electrical and optical properties we will give a hypothesis about the most probable mechanism. A close look to Fig. 3 reveals that at FA 900 °C and RTA 1000 °C 6 s, a considerable diffusion of Eu toward the interfaces of the gate oxide layer starts which culminates in strong interface decorations and large clusters up to 20 nm in the case of FA 1000 °C (Figs. 1 and 2). Concurrently, the rise phase of the EL intensity is more pronounced for high thermal budgets (Figs. 9 and 11). This leads at first to the question at which location excitable Eu^{3+} ions can be found in the oxide layer.

In Ref. 12, it was reported that luminescent Eu^{3+} ions are either finely dispersed in the oxide matrix or located close or at the Eu/Eu oxide cluster surface as Eu in the core of a cluster—independent of its oxidation state—is difficult to excite electrically. With increasing thermal budget, the number of luminescent Eu^{3+} ions decrease as the dispersed Eu^{3+} ions will diffuse toward the interfaces or toward the growing clusters. At the same time, the surface-to-volume ratio of the clusters decreases, and in turn a general decrease in EL intensity is observed with increasing annealing temperature. For 950 and 1000 °C, we assume that nearly all Eu^{3+} ions are located at the oxide interfaces or being part of the clusters, and that during the rise phase the excitation conditions will be improved for them.

[This article is copyrighted as indicated in the article. Reuse of AIP content is subject to the terms at: http://scitation.aip.org/termsconditions. Downloaded to] IP: 129.21.35.191 On: Sat, 20 Dec 2014 17:09:12

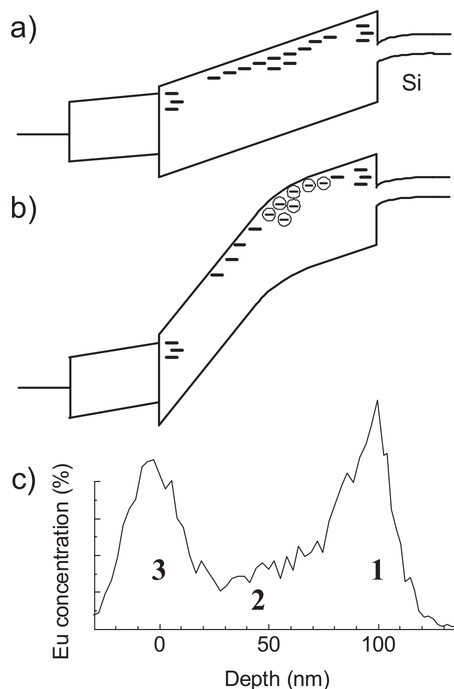

FIG. 15. Schematic band diagram of an Eu-implanted MOSLED under forward bias at the beginning of (a) and after considerable charge injection (b). The Eu profile for FA 1000 °C is given at the bottom (c).

The situation for the Eu-implanted MOSLED annealed with a high thermal budget at the beginning of charge injection (a) and in an advanced state of charge injection (b) is illustrated in Fig. 15. At the bottom, the RBS profile for FA 1000 °C is given (c) showing three different regions 1, 2, and 3 with Eu segregations at the interface regions 1 and 3 and large Eu/Eu oxide clusters in region 2. The capability of these clusters to trap electrons is indicated by an extended distribution of traps in the oxide layer. At the beginning of charge injection, these traps are assumed to be empty [Fig. 15(a)] or even positively charged. With increasing charge injection, more and more electrons will be trapped by the clusters which leads to a down bending of the band diagram between regions 2 and 3 because of the electric field between regions 1 and 2 is kept constant in order to ensure a constant injection current [Fig. 15(b)]. Thus the electric field between regions 2 and 3 is enhanced.

The effect on potential luminescence centers being located in the different Eu-rich regions is the following. It is assumed that Eu^{3+} ions in region 1 cannot be excited by the injected electrons as they do not have enough kinetic energy. According to Ref. 20, an acceleration distance in the order of 10–20 nm is needed before the energy distribution of the injected hot electrons reaches the equilibrium distribution. Considering the trapping of negative charges Eu^{3+} ions residing at the cluster surface or in the core of *negatively* charged clusters are also unsuitable candidates for causing the EL rise phase, as they are effectively screened from hot electrons by Coulomb repulsion. However, this mostly applies to clusters more close to the $Si-SiO_2$ interface. As the electric field increases toward the SiO_2-SiON interface due to band bending, a part of the clusters of region 2 is also located in the high field region. Eu^{3+} ions in region 3 and partly from region 2 profit from the enhanced local electric field in two aspects. First, the enhanced electric field causes a shift of the energy distribution of hot electrons to higher energies, which in turn increases the probability for an electron to excite an Eu^{3+} ion by impact excitation. Second, enhanced detrapping and field ionization may occur. In this scenario, most of the Eu^{3+} ions at the SiO_2-SiON interface or in the clusters are blocked by trapped electrons in the close vicinity. Higher electric fields shift the balance between charge trapping and detrapping to a lower occupancy of the traps.[19] As a consequence, less and less Eu^{3+} ions are blocked by electrons which results in an increase in EL intensity. The question if the high electric field may trigger the direct transformation $Eu^{2+} \rightarrow Eu^{3+}$, we tend to negate as in some cases an increase in both the blue and red EL lines is observed.[24]

However, the advantageous situation for Eu^{3+} ions in the high field region is not stable in the long term. In unimplanted MOS structures, it was found that the trap generation rate starts to increase continuously with increasing kinetic energy of the electrons if a threshold value of 2.3 eV is exceeded.[25] However, such values are already achieved for electric fields as low as 4 MV cm^{-1},[20] whereas the local electric field for Eu-implanted MOSLEDs can easily reach the order of 10 MV cm^{-1} (Fig. 5). As a consequence, there is a continuous creation of traps during charge injection, especially in region 3, and thus an additional and increasing electron trapping by these traps which counteract the activation of blocked Eu^{3+} ions. Because of this degradation process, Eu-implanted MOSLEDs are also subjected to the same EL quenching like other RE-implanted MOSLEDs, albeit in a decelerated manner.

The EL rise phenomenon is clearly correlated with the presence of large clusters in the bulk, with negative charge trapping during charge injection and with the existence of Eu segregations at the interfaces of the gate oxide layer. However, correlation is not yet a proof, for which reason the suggested scenario is a model that explains the observed phenomena based on the aforementioned correlations but which still requires a more detailed experimental validation. Nevertheless, the presented model is the best someone can conclude from the existing experimental data.

IV. SUMMARY

In summary, the anomalous wear-out phenomena of Eu-implanted MOSLEDs were investigated. In contrast to other RE-implanted MOSLEDs, the EL intensity dependence on the injected charge shows an unusual rise phase before quenching processes start to dominate. The rise phase is more pronounced for higher thermal budgets but is accompanied by a decrease in the overall EL intensity. This dependence was correlated with the microstructural development which had been traced by TEM, RBS, and NRA measurements. According to this a strong increase in Eu/Eu oxide cluster sizes, a massive diffusion of Eu toward the gate oxide interfaces and a decrease in the hydrogen concentration at the SiO_2-SiON interface was observed with increasing thermal budgets, e.g., with increasing annealing temperature

[This article is copyrighted as indicated in the article. Reuse of AIP content is subject to the terms at: http://scitation.aip.org/termsconditions. Downloaded to] IP: 129.21.35.191 On: Sat, 20 Dec 2014 17:09:12

and/or increasing annealing time. It was found that the charge trapping behavior is composed of two components: a general part controlled by the annealing procedure and the hydrogen content and thus indirectly by the presence of the SiON layer, and an Eu-dependent part which is characterized by additional electron trapping under charge injection. Based on these correlations, we suppose that the EL rise phase is caused by Eu^{3+} ions being either located at the SiO_2-SiON interface or being part of clusters close to that interface. It is assumed that their excitation cross section increases because of the higher kinetic energy of the hot electrons due to the enhanced local electric field during negative charge trapping in the bulk. Furthermore, some of the Eu^{3+} ions which are blocked by electrons in nearby traps can additionally attribute to the observed EL if the number of blocking and trapped electrons decreases due to an enhanced detrapping under high electric fields.

[1]M. Oehme, J. Werner, E. Kasper, M. Jutzi, and M. Berroth, Appl. Phys. Lett. **89**, 071117 (2006).
[2]S. G. Johnson, P. R. Villeneuve, S. Fan, and J. D. Joannopoulos, Phys. Rev. B **62**, 8212 (2000).
[3]A. Liu, R. Jones, L. Liao, D. Samara-Rubio, D. Rubin, O. Cohen, R. Nicolaescu, and M. Paniccia, Nature (London) **427**, 615 (2004).
[4]A. Sciuto, S. Libertino, S. Coffa, and G. Coppola, Appl. Phys. Lett. **86**, 201115 (2005).
[5]S. Wang, A. Eckau, E. Neufeld, R. Carius, and Ch. Buchal, Appl. Phys. Lett. **71**, 2824 (1997).
[6]F. Lu, R. Carius, A. Alam, M. Heuken, and C. Buchal, J. Appl. Phys. **92**, 2457 (2002).
[7]M. E. Castagna, S. Coffa, M. Monaco, A. Muscara, L. Caristia, S. Lorenti, and A. Messina, Mater. Sci. Eng., B **105**, 83 (2003).
[8]F. Iacona, D. Pacifici, A. Irrera, M. Miritello, G. Franzò, F. Priolo, D. Sanfilippo, G. Di Stefano, and P. G. Fallica, Appl. Phys. Lett. **81**, 3242 (2002).
[9]J. M. Sun, W. Skorupa, T. Dekorsy, M. Helm, L. Rebohle, and T. Gebel, J. Appl. Phys. **97**, 123513 (2005).
[10]J. M. Sun, W. Skorupa, T. Dekorsy, M. Helm, L. Rebohle, and T. Gebel, Appl. Phys. Lett. **85**, 3387 (2004).
[11]S. Prucnal, J. M. Sun, W. Skorupa, and M. Helm, Appl. Phys. Lett. **90**, 181121 (2007).
[12]L. Rebohle, J. Lehmann, S. Prucnal, A. Kanjilal, A. Nazarov, I. Tyagulskiib, W. Skorupa, and M. Helm, Appl. Phys. Lett. **93**, 071908 (2008).
[13]A. N. Nazarov, I. Osiyuk, I. Tyagulskii, V. Lysenko, S. Prucnal, J. Sun, W. Skorupa, and R.A. Yankov, J. Lumin. **121**, 213 (2006).
[14]A. N. Nazarov, I. P. Tyagulskyy, S. I. Tyagulskiy, L. Rebohle, W. Skorupa, J. Biskupek, and U. Kaiser, Physica E (Amsterdam) **41**, 902 (2009).
[15]J. F. Ziegler and J. P. Biersack, *Stopping and Range of Ions in Matter* (Pergamon Press, New York, 2003).
[16]A. Stoffel, A. Kovács, W. Kronast, and B. Müller, J. Micromech. Microeng. **6**, 1 (1996).
[17]*Instabilities in Si devices*, edited by G. Barbottin and A. Vapaille (Elsevier Science, Amsterdam, 1986).
[18]J. M. Sun, L. Rebohle, S. Prucnal, M. Helm, and W. Skorupa, Appl. Phys. Lett. **92**, 071103 (2008).
[19]D. J. DiMaria, E. Cartier, and D. Arnold, J. Appl. Phys. **73**, 3367 (1993).
[20]M. V. Fischetti, D. J. DiMaria, S. D. Brorson, T. N. Theis, and J. R. Kirtley, Phys. Rev. B **31**, 8124 (1985).
[21]G. H. Dieke, *Spectra and Energy Levels of Rare Earth Ions in Crystals* (Interscience, New York, 1968).
[22]V. A. Gritsenko, H. Wong, J. B. Xu, R. M. Kwok, I. P. Petrenko, B. A. Zaitsev, Y. N. Morokov, and Y. N. Novikov, J. Appl. Phys. **86**, 3234 (1999).
[23]L. Rebohle, J. von Borany, H. Fröb, and W. Skorupa, Appl. Phys. B: Lasers Opt. **70**, 1 (2000).
[24]S. Tyagulskiy, I. Tyagulskiy, A. Nazarov, V. Lysenko, L. Rebohle, J. Lehmann, and W. Skorupa, Microelectron. Eng. **86**, 1954 (2009).
[25]D. J. DiMaria and M. Fischetti, in *Excess Electrons in Dielectric Media*, edited by C. Ferradini and J. P. Jay-Gerin (CRC, Boca Raton, FL, 1991), p. 315.

[This article is copyrighted as indicated in the article. Reuse of AIP content is subject to the terms at: http://scitation.aip.org/termsconditions. Downloaded to] IP: 129.21.35.191 On: Sat, 20 Dec 2014 17:09:12